Electronic Supplementary Material (ESI) for Materials Advances.

Supplementary Information

Fabrication of thin solid electrolytes containing a small volume of an Li_3OCl-type antiperovskite phase by RF magnetron sputtering

Stephen J Turrell[a,b], Hyeon Jeong Lee[a,b,c], Marco Siniscalchi[a,b], Sudarshan Narayanan[a,b], Mauro Pasta[a,b], Susannah C Speller[a], Chris R M Grovenor[a,b]

[a]*Department of Materials, University of Oxford, Parks Road, Oxford OX1 3PH, United Kingdom*

[b]*The Faraday Institution, Harwell Campus, Quad One, Becquerel Avenue, Didcot OX11 0RA, United Kingdom*

[c]*Division of Chemical Engineering and Bioengineering, Kangwon National University, 1 Kangwondaehak-gil, Chuncheon 24341, Republic of Korea*

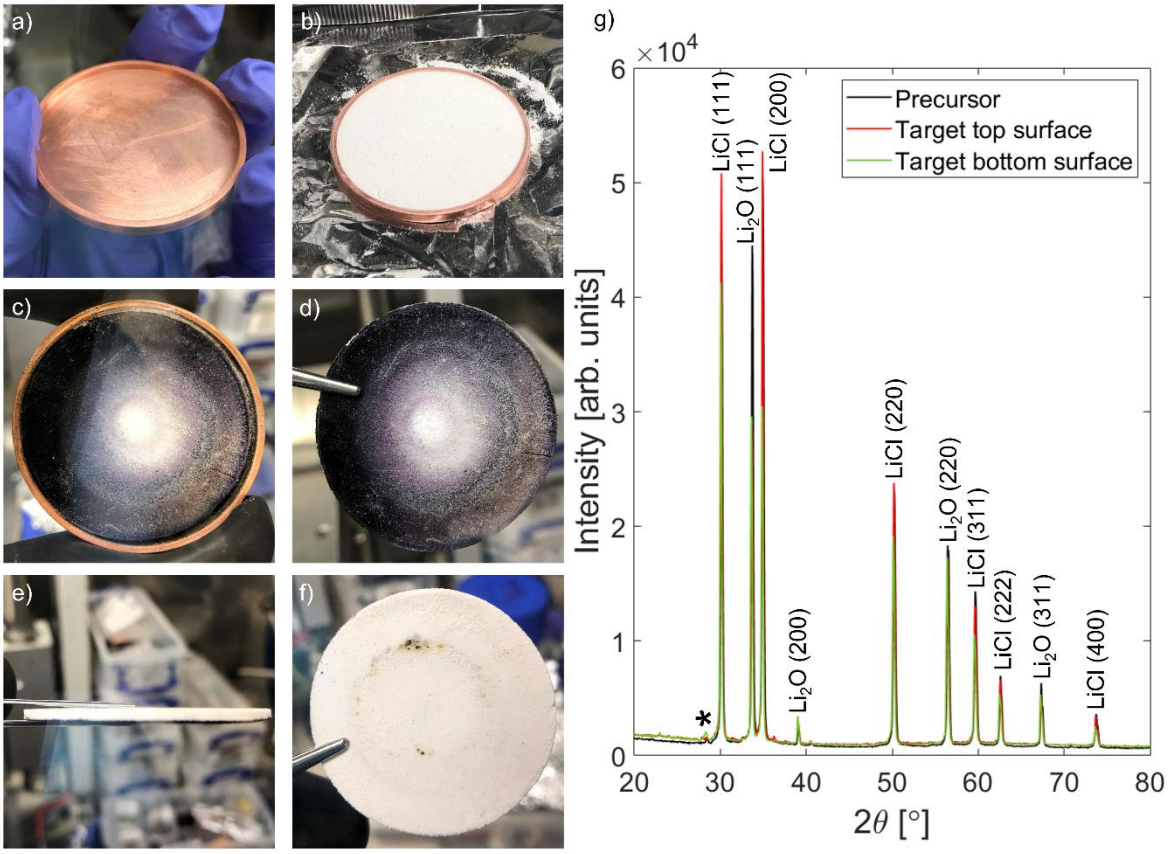

Figure S1 Appearance and crystallographic properties of the Li_2O + LiCl target before and after sputtering. The photographs show a) the copper powder target holder, b) the powder target before sputtering, c) and d) the top surface of the target after the deposition process, e) a side view of the target after deposition, and f) the bottom surface of the target after deposition. The XRD patterns in g) are from the Li_2O + LiCl precursor powder mixture and powder samples taken from the top surface and bottom surface regions of the target after deposition. The peak marked * corresponds to an impurity phase thought to be KCl.

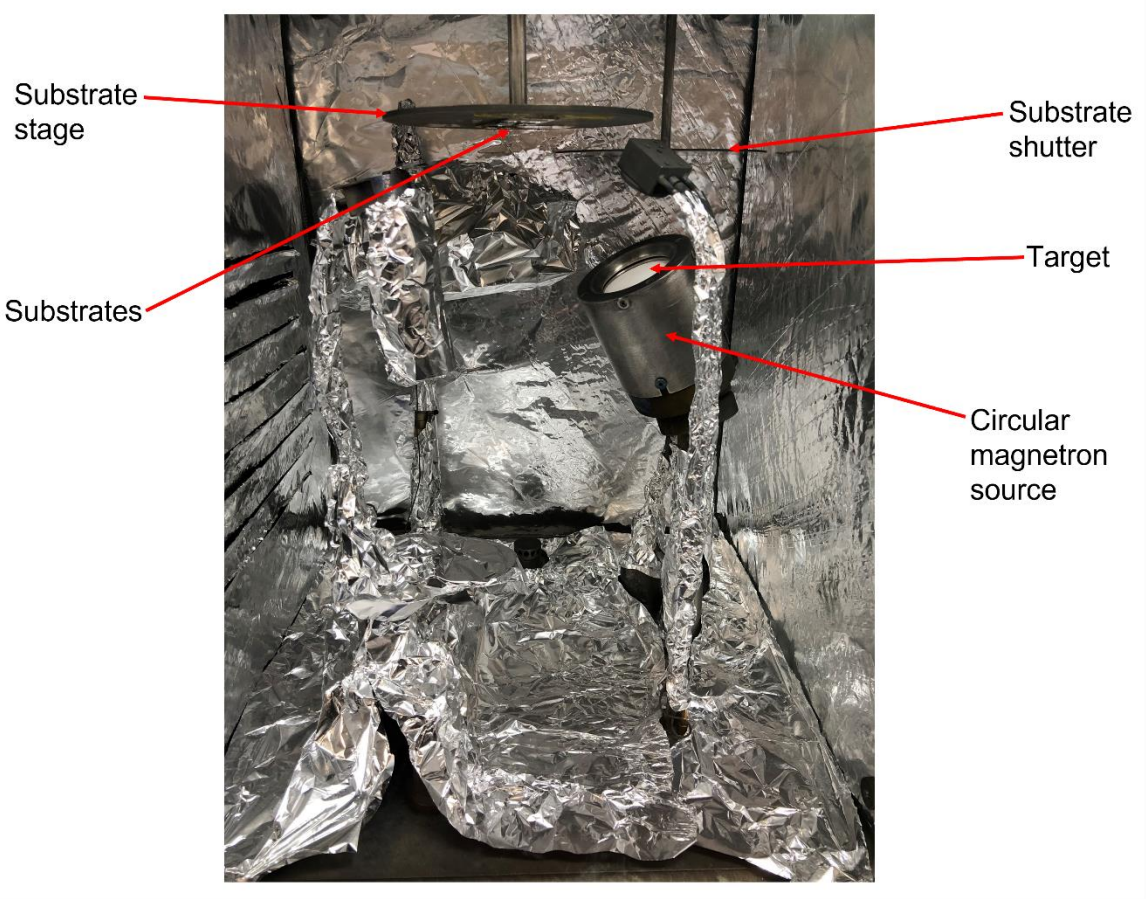

Figure S2 Photograph of the MB EVAP (MBraun) PVD system used for thin film deposition. This photograph was taken prior to deposition, with the substrates and powder target loaded.

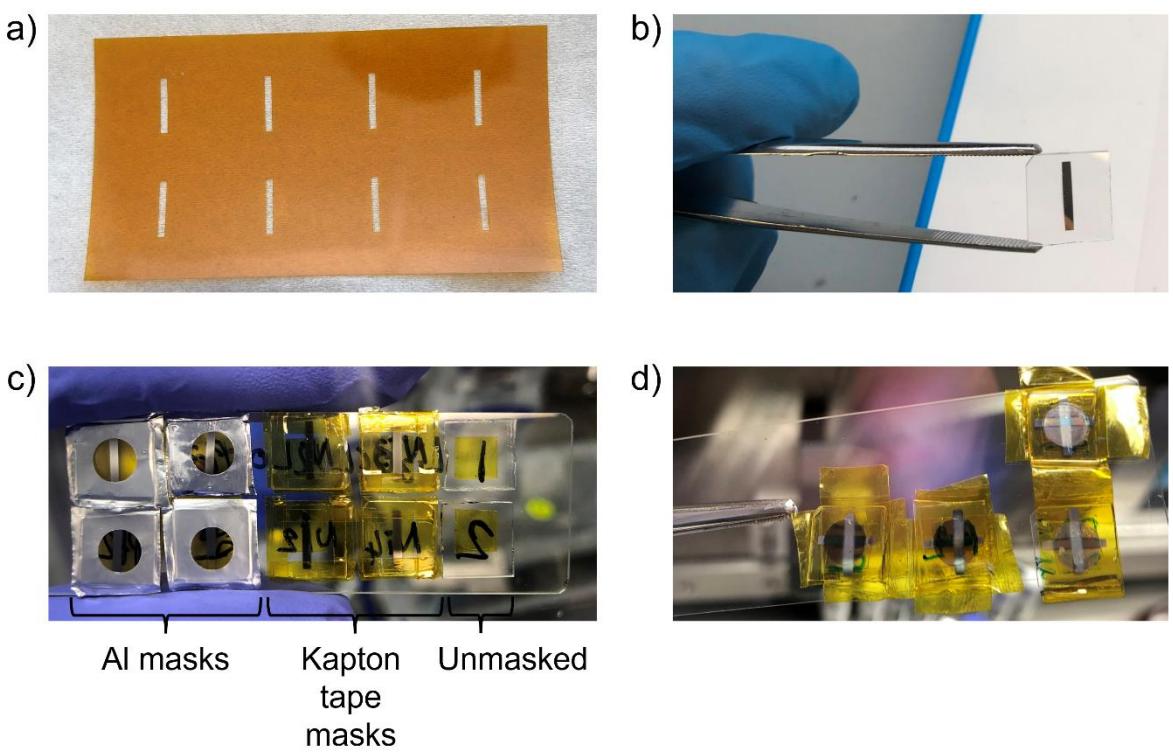

Figure S3 Photographs of the stages of fabrication of glass/metal/electrolyte/metal samples for impedance measurements on electrolyte films deposited from the Li_2OHCl target: a) Kapton film shadow masks for electrical contact deposition, b) metal bottom contact on glass substrate, c) samples masked for electrolyte film deposition, and d) after deposition of the top metal contact (oriented at ~90° to the bottom contact).

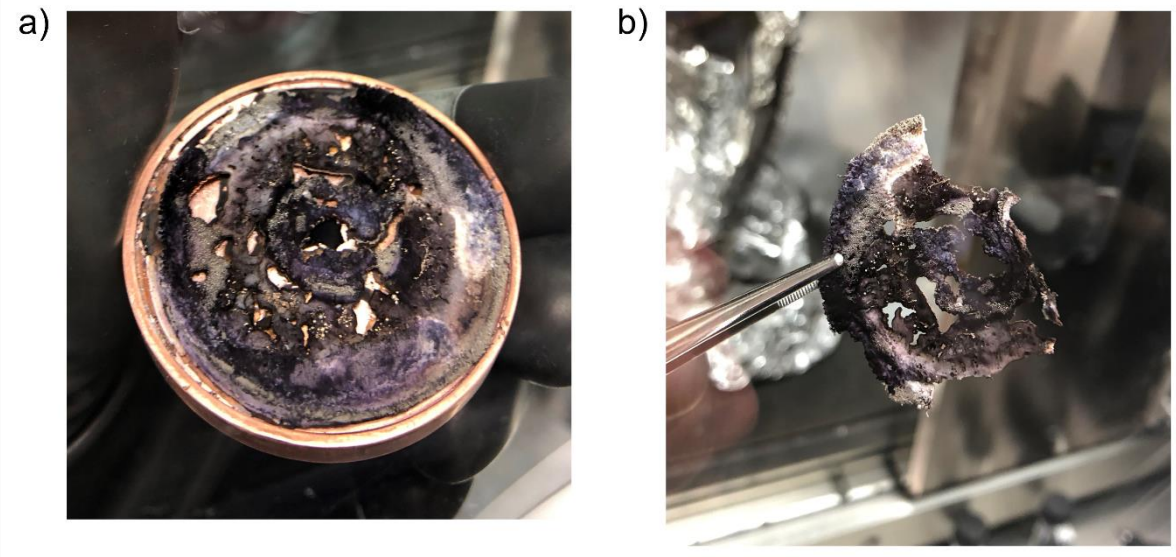

Figure S4 Appearance of the Li_2OHCl target after sputter deposition: a) target in the copper holder and b) fragment of sintered/melted powder removed from the copper holder.

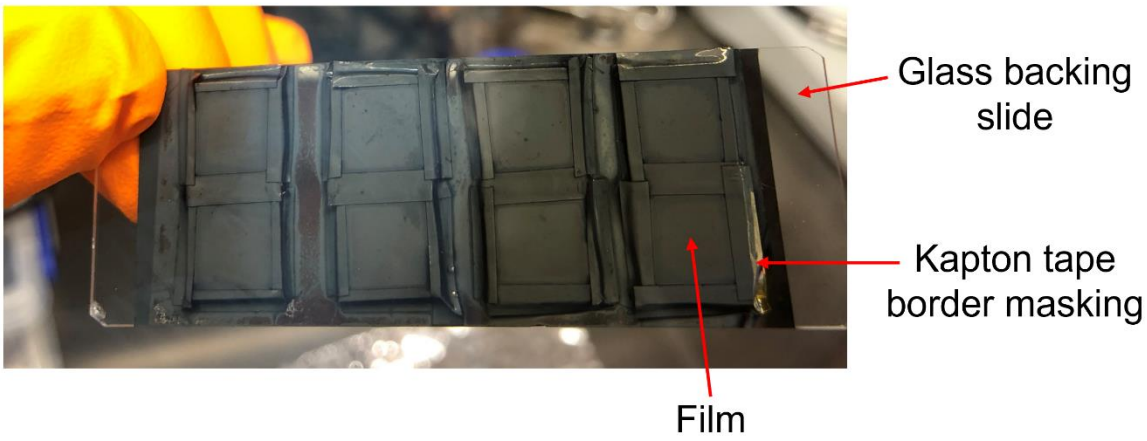

Figure S5 Photograph of films deposited from an Li_2O + LiCl target onto nickel-coated glass substrates.

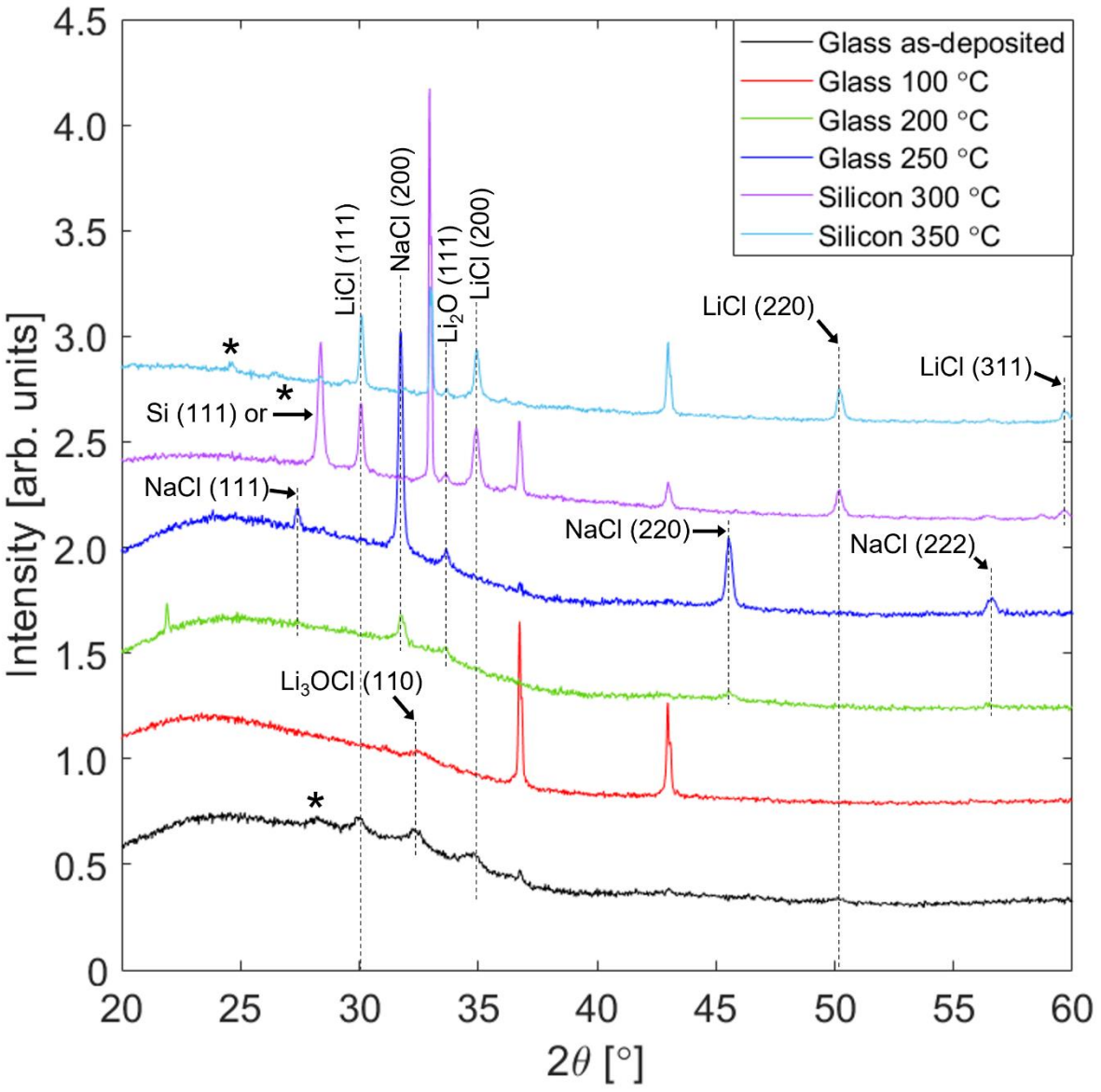

Figure S6 XRD patterns of films deposited from Li_2O + LiCl targets onto glass and silicon substrates and annealed at 100 °C and 200 °C for 1 hour (glass) and 300 °C and 350 °C for 1 hour (silicon) to investigate the temperature stability of the Li_3OCl phase. Samples on silicon substrates were chosen for the highest temperature annealing to avoid any influences from sodium on the Li_3OCl phase stability. Also plotted for comparison are the patterns from as-deposited and 250 °C annealed films on glass substrates, which were shown previously in Figure 2. Peaks marked * correspond to impurity phases from the precursor mixture such as KCl. Unlabelled peaks are from the substrate or sample holder; the differing intensities of holder peaks are due to differences in lateral positioning of the samples within the holder.

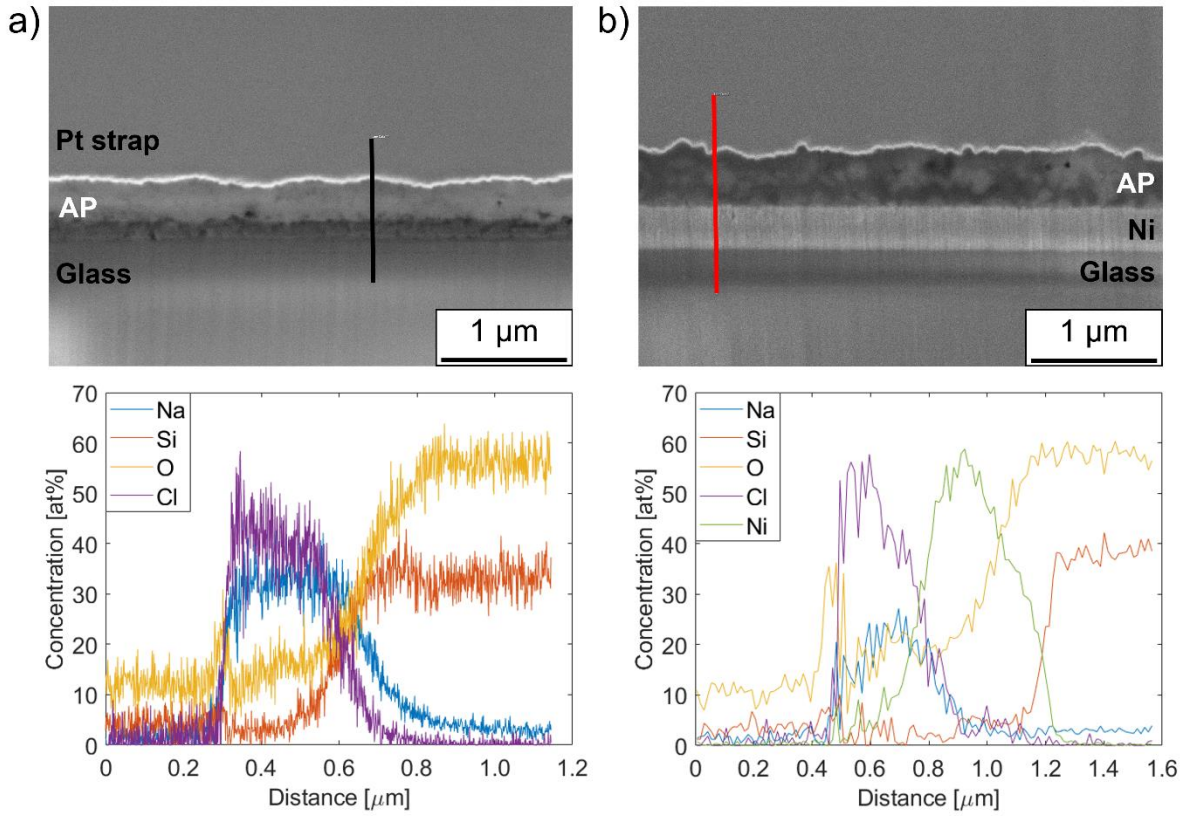

Figure S7 EDX profiles for sodium, silicon, oxygen, chlorine and nickel measured on the cross-sections of films annealed at 250 °C for 1 hour on a) uncoated glass and b) nickel-coated glass substrates. The black and red lines drawn on the SEM micrographs show the respective locations of the line scans, which started above the film surface and ended within the substrate. While the elemental concentrations are given as atomic percentages, these do not account for the lithium content of the films and are therefore only valid for determining relative concentrations.

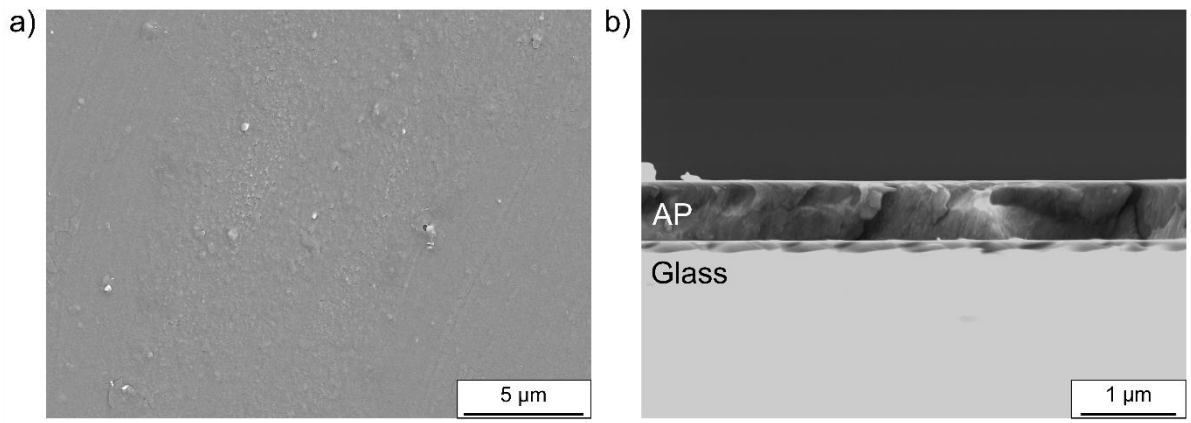

Figure S8 SEM micrographs of a film deposited from an Li_2OHCl target onto a glass substrate, taken after performing impedance measurements between 25 and 100 °C. The film surface is shown in a), while b) is a view of the cross-section produced by fracturing the sample. In the cross-sectional view, the image is slightly distorted due to charging by the electron beam. The region imaged does not contain the electrical contacts used for impedance measurements.

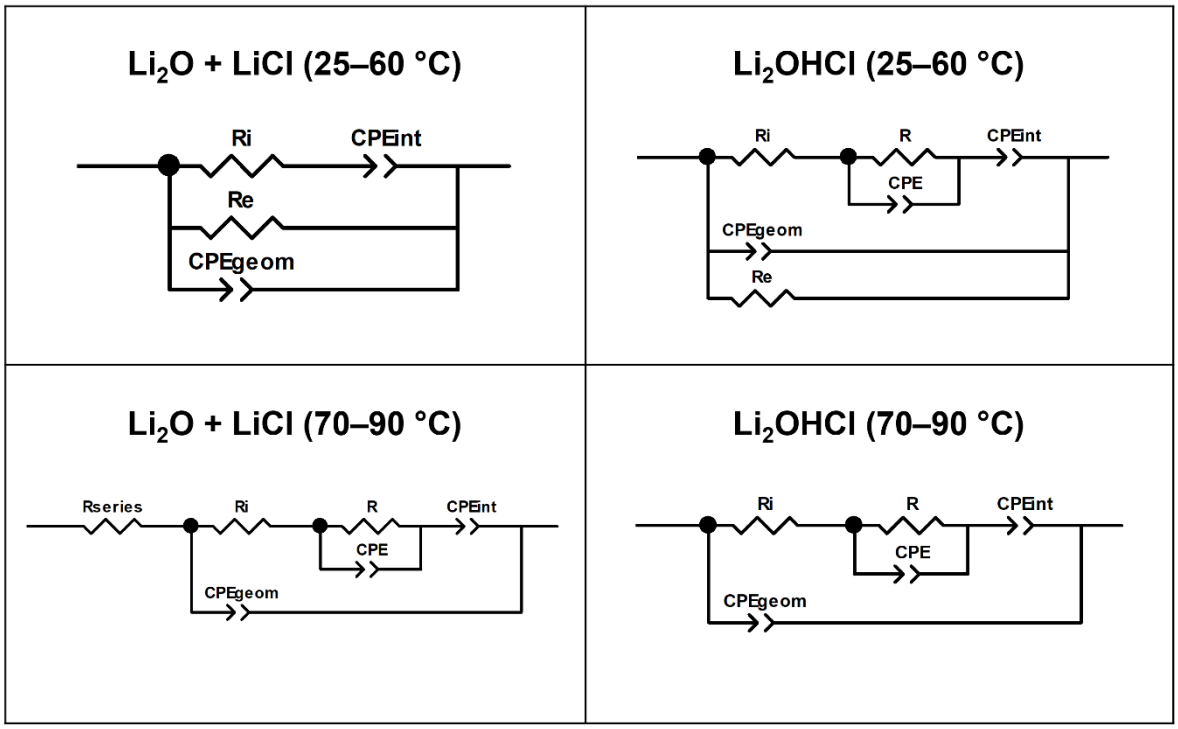

Figure S9 Diagrams of the equivalent circuits used to model the Nyquist plots in Figure 7 a) and b). 'Ri' is the ionic resistance, 'Re' is the electronic resistance, 'R' is another resistance component (e.g. grain boundary resistance), Rseries is a series resistance (e.g. due to the resistance of the electrical contacts), 'CPEint' is the interfacial capacitance, 'CPEgeom' is the geometric capacitance and 'CPE' is the capacitance of the element associated with the resistance 'R'.

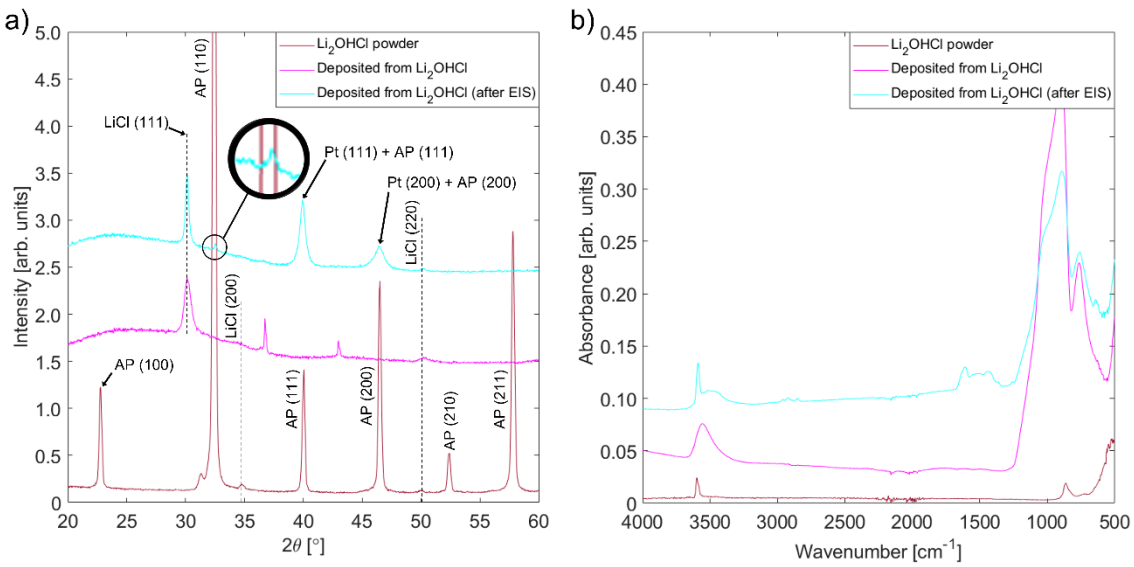

Figure S10 Characterization of films deposited from an Li_2OHCl target before and after performing impedance measurements between 25 and 100 °C. XRD patterns are shown in a), while b) shows corresponding FT-IR spectra. Data from characterization of a Li_2OHCl powder sample are also included for comparison. On the XRD patterns, peaks marked 'AP' correspond to the Li_3OCl/Li_2OHCl antiperovskite phase. Unlabelled peaks are from the sample holder; the differing intensities of holder peaks are due to differences in lateral positioning of the samples within the holder. The large circle contains an enlarged view of a small AP (110) peak.

Table S1 Impedance contact overlap areas used in ionic conductivity calculations.

Sample	Electrical contact overlap area / cm^2	Method of area measurement
Film deposited from Li_2O + LiCl target	0.016218229	PFIB used for SEM imaging of top contact in surface view. Circular measurement tool used to measure diameter of top contact, allowing calculation of its area (which is equal to the overlap area).
Film deposited from Li_2OHCl target	0.0183	SEM used to image contacts in surface view. Widths of top and bottom contacts measured as close to the region of overlap as possible and multiplied together to obtain the overlap area.